Observation of magnetic octupole order producing anomalous Hall effect by X-ray magnetic circular dichroism

The anomalous Hall and thermoelectric (Nernst) effects in magnetic materials have recently been attracting considerable attention because of their potential applications to spintronics, energy harvesting, and magnetic sensing, for example. Thus far, these functionalities have mostly been studied in ferromagnets since it might be considered that large uniform magnetization is necessary to produce strong effects. On the other hand, large anomalous Hall and Nernst effects have recently been found in an antiferromagnetic metal, Mn_3Sn [1]. Mn_3Sn has a two-dimensional kagome lattice, and the total magnetization is vanishingly small (~0.002 μ_B/Mn) owing to the triangular antiferromagnetic spin structure, as shown in Fig. 1(a). Therefore, the mechanism of these large responses is expected to be completely different from that of conventional ferromagnets, where the magnitude of anomalous Hall effect is roughly proportional to the magnetization. The origin of anomalous Hall effect is currently understood to be a novel type of order parameter called the cluster magnetic octupole, that, in principle, breaks time reversal symmetry (TRS) without net magnetization [2]. However, the presence of magnetic octupole order has not been well established because of the lack of a suitable experimental approach. To solve this problem, we have applied X-ray magnetic circular dichroism (XMCD) to Mn_3Sn, since the circularly polarized X-ray can generally couple with the TRS-broken order [3]. Indeed, recent theoretical studies [4,5] indicate the detection of the XMCD signal in a triangular antiferromagnet such as Mn_3Sn through the magnetic dipole term called the T_z term.

Figure 1(a) shows a schematic of the experimental setup for XMCD measurement. The experiment was performed at SPring-8 **BL25SU**. The right and left circularly polarized X-ray beams are irradiated to the (0001) plane of the crystal. The angle between the magnetic field and the (0001) plane is defined as θ. The direction of the X-ray beam is tilted 10 more degrees from the field direction. Figure 1(b) shows the typical XMCD and XAS spectra of Mn_3Sn for $B = 1$ T and $T = 300$ K. As can be seen in the figure, clear positive and negative XMCD signals were observed at L_3 and L_2 edges, and this feature is indeed opposite to those of conventional ferromagnetic Mn compounds, where the XMCD signal is negative and positive for L_3 and L_2 edges, respectively. The observed XAS shows broad absorption peaks similarly to the other Mn metallic compounds, indicating the formation of a dispersive itinerant band of Mn *d* orbitals.

The main panel of Fig. 2 shows the field orientation dependence of XMCD for B = 1 T. As can be seen in the figure, the signal intensity is anisotropic. Since the anisotropy of magnetization with B = 1 T is small (see the right inset), the intensity variation of XMCD cannot be explained by the magnetization anisotropy. The left inset of Fig. 2 shows the XMCD spectrum for B = 0 T, i.e., the residual spontaneous component. The intensity and shape of this XMCD spectrum are mostly identical to those for B = 1 T, and this feature also cannot be explained by the magnetization process, where the magnetization increases about 4-fold between 0 and 1 T with a linear slope, as shown in the right inset. These features clearly show that the present XMCD is decoupled from the magnetization behavior, indicating that the origin of the present XMCD is completely different from that of the conventional XMCD, in which the XMCD response is proportional to the static magnetization.

To reveal the origin of the present XMCD signal, we performed a theoretical calculation of the XMCD spectrum (Figs. 3(a)-(d)). Thick blue lines show the total XMCD signal, and thin magenta, light green, and orange lines correspond to individual XMCD contributions from spin sublattices A, B, and C, respectively. In Fig. 3(a), a clear XMCD signal appears even though the total

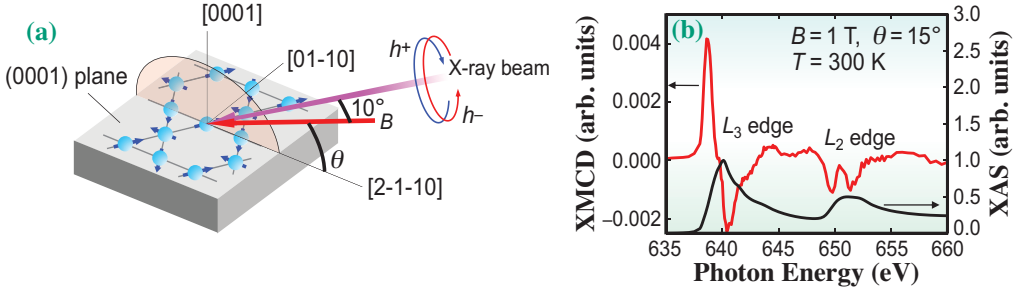

Fig. 1. **(a)** Schematic of experimental setup of XMCD measurement. **(b)** Typical XMCD (left axis) and XAS (right axis) spectra of Mn_3Sn for B = 1 T (θ = 15°) and T = 300 K. [3]

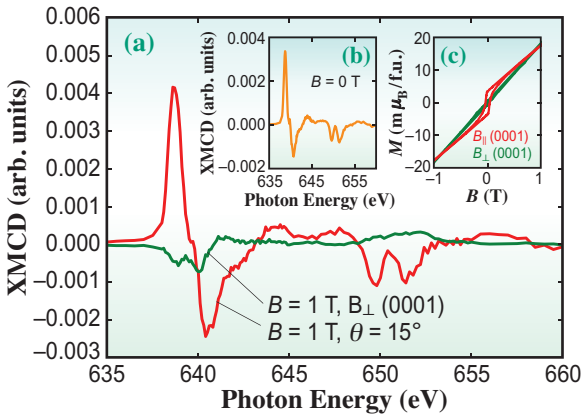

Fig. 2. **(a)** Magnetic field orientation dependence of XMCD signal. Both spectra are measured at 1 T. **(b)** XMCD spectrum for B = 0 T. **(c)** Field orientation dependence of magnetization curve. [3]

spin moment is zero. On the other hand, in Fig. 3(b), individual XMCD contributions compensate each other and the total XMCD is zero. Although the two magnetic structures in Figs. 3(a) and 3(b) have a triangular antiferromagnetic structure, the difference is the sign of spin chirality, i.e., the rotation direction of spin moment. For the inset of Fig. 3(a), the spin moment rotates counterclockwise (–120°) when the position of spin is changed on the triangular Mn sites clockwise as A to C. In this case, the spin chirality is negative. On the other hand, in Fig. 3(b), the spin direction is clockwise (+120°) for the same operation, i.e., the spin chirality is positive. Importantly, from the group theory consideration, the TRS-broken cluster magnetic octupole only appears when the spin chirality is negative [2]. Thus, our model calculation shows the complete correspondence between the appearance of XMCD and the cluster octupole order. Note that the magnetic structure shown in Fig. 3(a) is realized in Mn_3Sn, while that in Fig. 3(b) is a fictitious magnetic structure for comparison.

The additional model calculations (Figs. 3(c) and 3(d)) also show that the unconventional XMCD behavior observed in the experiment (field-strength-independent in-plane XMCD signal, and different spectral signs and shapes between parallel and perpendicular field directions) can be reproduced by our model. Figure 3(c) shows the calculated XMCD for the in-plane field configuration with a slight in-plane magnetic moment of ~18 $m\mu_B$ corresponding to $B_{||} \approx 1$ T. The spectral shape and intensity are mostly identical for B = 0 T. This means that the origin of the present XMCD is not the field-induced moment, but the inverse triangular magnetic structure itself, which is mostly preserved in such a weak field region as shown in the inset. When the magnetic field is perpendicular to the kagome plane (Fig. 3(d)), a weak XMCD signal from a paramagnetic contribution due to spin canting was expected, and this is also consistent with the experimental observation.

In summary, we have demonstrated that the unconventional XMCD in Mn_3Sn arises from the inverse triangular antiferromagnetic structure characterized by the TRS-broken cluster magnetic octupole order. Although the XMCD detection of the magnetic octupole moment was predicted theoretically, our experimental observation shows the efficiency of XMCD in detecting ferroic higher-rank multipole order. This result may increase the variety of applicable targets of X-ray magnetic spectroscopy.

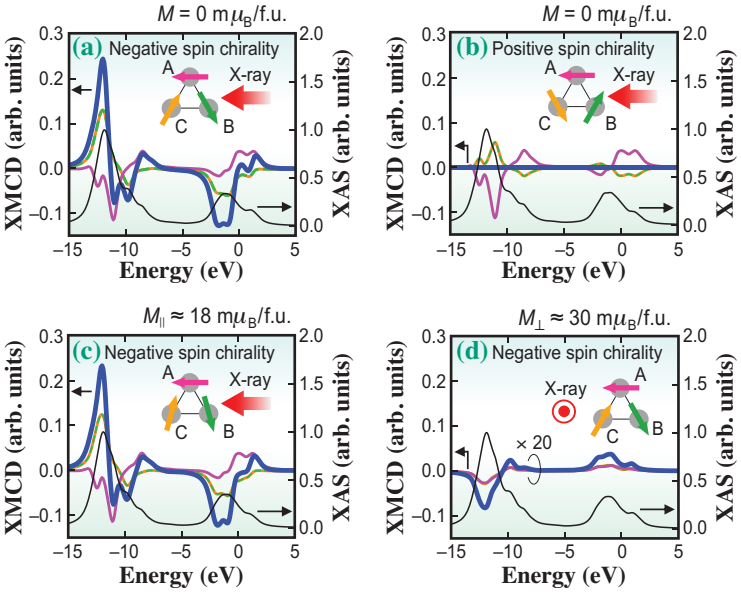

Fig. 3. Calculated XMCDs for different field and X-ray configurations. **(a,b)** Spin chirality dependence of XMCD signal. **(c,d)** Calculated XMCDs for parallel and perpendicular field (and X-ray) configurations, respectively. [3]

Motoi Kimata[a,*], Norimasa Sasabe[b] and Tetsuya Nakamura[a,b]

[a] Institute for Materials Research, Tohoku University
[b] Japan Synchrotron Radiation Research Institute (JASRI)

*Email: motoi.kimata.b4@tohoku.ac.jp

References

[1] S. Nakatsuji *et al.*: Nature **527** (2015) 212.
[2] M.-T. Suzuki *et al.*: Phys. Rev. B **95** (2017) 094406.
[3] *M. Kimata, N. Sasabe, K. Kurita, Y. Yamasaki, C. Tabata, Y. Yokoyama, Y. Kotani, M. Ikhlas, T. Tomita, K. Amemiya, H. Nojiri, S. Nakatsuji, T. Koretsune, H. Nakao, T.-H. Arima, and T. Nakamura: Nat. Commun.* ***12*** *(2021) 5582.*
[4] Y. Yamasaki *et al.*: J. Phys. Soc. Jpn. **89** (2020) 083703.
[5] *N. Sasabe, M. Kimata and T. Nakamura: Phys. Rev. Lett. 126 (2021) 157402.*